J|A|C|S
ARTICLES
Published on Web 02/02/2002

Supramolecular Gold Nanoparticles for the Redox Recognition of Oxoanions: Syntheses, Titrations, Stereoelectronic Effects, and Selectivity†

Agnès Labande, Jaime Ruiz, and Didier Astruc*

Contribution from Laboratoire de Chimie Organique et Organométallique, UMR CNRS No. 5802, Université Bordeaux I, 33405 Talence Cedex, France

Received September 6, 2001

Abstract: Stable, CH_2Cl_2-soluble mixed dodecanethiol/(amidoferrocenyl)alkanethiol (AFAT) gold colloids were synthesized by ligand substitution reactions from Brust's dodecanethiol gold colloids and the AFAT ligands to study the recognition and titration of oxoanions. Gold colloids were obtained with various chain lengths (C_{11} and C_6 chains) of the AFAT ligand and different proportions of AFAT ligands in the colloids. Modification of the amidoferrocenyl structure [replacement of the free C_5H_5 ferrocene ring by C_5Me_5 (Cp*) or $C_5H_4COCH_3$] has been achieved to investigate the stereoelectronic effects on the recognition. The cyclic voltammetry of these colloids in CH_2Cl_2 on Pt electrode shows a reversible $Fe^{II/III}$ wave with some adsorption. With AFAT ligands, a new, less electrochemically reversible wave (with some adsorption) at a potential 220 ± 20 mV less positive than that of the initial wave appears upon titration of [*n*-Bu_4N][H_2PO_4], and the initial wave completely disappears after addition of 1 equiv of anion, which allows its titration. The potential shift does not depend on the AFAT proportion nor on its chain length but is reduced with Cp* and enhanced with $C_5H_4COCH_3$, showing the key role of the hydrogen bonding between the −NH− amido group and a terminal oxygen atom of the oxoanions. According to the Echegoyen−Kaifer model, the potential shift leads to the ratio $K_{(+)}/K_{(0)}$ of apparent association constants. In the presence of both [*n*-Bu_4N][HSO_4] and [*n*-Bu_4N]-Cl, a shift of the initial wave (rather than its replacement) allows an easy titration, ideally with 20-Fc. Upon addition of [*n*-Bu_4N][HSO_4] alone, a weak wave shift (30 mV) of the colloids is also observed, allowing the titration of the HSO_4^- anion by the colloids containing a low percentage of AFAT ligand. The Echegoyen−Kaifer model provides access to the apparent association constant $K_{(+)}$ in this case for which the interaction between the anion and the neutral form of the host is not significant. With the $C_5H_4COCH_3$ modification of the amidoferrocenyl branch, a new wave appears at a potential 70 mV more positive than the initial wave, signifying a stronger interaction with this modified ligand than with the parent AFAT ligand. These colloids favorably compare with ferrocenyl dendrimers in terms of rapid synthesis and selectivity of $H_2PO_4^-$ over HSO_4^- and with gold surfaces for the recognition of HSO_4^-.

Introduction

Among supramolecular materials,[1] colloids are excellent candidates for sensors[2] especially when redox recognition is involved.[3] The discovery by Brust[4] of stable, very well defined alkanethiol-stabilized gold nanoparticles[5] with narrow polydispersities has led to a new field of research. We wished to combine the effect of the topography of alkanethiol−gold nanoparticles and the supramolecular properties of their redox-active termini for their use as exo-receptors[1a] for the recognition of oxoanions.[6] To reach this goal, we have synthesized new

* Corresponding author. E-mail: d.astruc@lcoo.u-bordeaux.fr.

† Abbreviations: AFAT, 11-(amidoferrocenyl)-1-undecanethiolate (**1**); Fc, ferrocenyl; 20-Fc, mixed gold colloids containing 80% dodecanethiolate ligands and 20% AFAT ligands **1**, etc.; 18-Fc (C_6), mixed gold colloids containing 82% dodecanethiolate ligands and 18% 6-(amidoferrocenyl)-1-hexanethiolate ligands **6**; Cp*, η^5-C_5Me_5; 25-Fp*, mixed gold colloids containing 75% dodecanethiolate ligands and 25% AFAT ligands modified with Cp*, i.e. 11-(1-amido,1′-pentamethylferrocenyl)-1-undecanethiol, **7**; 6-FcAc, mixed gold colloids containing 94% dodecanethiolate ligands and 6% AFAT ligand modified with η^5-C_5H_4COMe, i.e. 11-(1-amido,1′-acetylferrocenyl)-1-undecanethiol, **15**; CV, cyclic voltammetry or cyclic voltammogram.

(1) Lehn, J.-M. *Supramolecular Chemistry: Concepts and Perspectives*; VCH: Weinheim, Germany, 1995. (b) Kumar, A.; Arbott, N. L.; Kim, E.; Biebuyck, A.; Whitesides, G. M. *Acc. Chem. Res.* **1995**, *28*, 219.

(2) (a) Fitzmaurice, D.; Rao, S. N.; Preece, J.; Stoddart, J. F.; Wenger, S. Zaccheroni, N. *Angew. Chem., Int. Ed.* **1999**, *38*, 1147. (b) Sampath, S.; Lev, O. *Adv. Mater*. **1997**, *9*, 410. (d) Boal, A. K.; Rotello, V. M. *J. Am. Chem. Soc*. **1999**, *121*, 4914. (e) Niemz, A.; Rotello, V. M. *Acc. Chem. Res*. **1999**, *32*, 44. (f) Elghanian, R.; Storhoff, J. J.; Mucic, R. C.; Letsinger, R. L.; Mirkin, C. A. *Science* **1997**, *277*, 1078. (g) Shenton, W.; Davis, D. A.; Mann, S. *Adv. Mater*. **1999**, *119*, 11132.

(3) (a) Astruc, D. *Electron-Transfer and Radical Processes in Transition-Metal Chemistry*; VCH: New York, 1995; Chapter 2. (b) *Electron Transfer in Chemistry*; Balzani, V., Ed.; Wiley-VCH: Weinheim, Germany, 2001; Vol. 2, Section II.

(4) (a) Brust, M.; Walker, M.; Bethell, D.; Schiffrin, D. J.; Whyman, R. *J. Chem. Soc. Chem. Commun.* **1994**, 801. (b) Brust, M.; Fink, J.; Bethell, D.; Schiffrin, D. J.; Kiely, C. *Chem. Commun.* **1995**, 1655.

(5) For reviews on colloids previous to Brust's discovery, see: (a) Schmid, G. *Chem. Rev*. **1992**, *92*, 1709. (b) Bradley, J. S. In *Clusters and Colloids*; Schmid, G., Ed.; VCH: Weinheim, Germany, 1995; Chapter 6. (c) See also: Schmid, G.; Chi, L. F. *Adv. Mater*. **1998**, *18*, 515.

(6) (a) Valério, C.; Fillaut, J.-L.; Ruiz, J.; Guittard, J.; Blais, J.-C; Astruc, D. *J. Am. Chem. Soc*. **1997**, *119*, 2588. (b) Valério, C.; Alonso, E.; Ruiz, J.; Blais, J.-C.; Astruc, D. *Angew. Chem., Int. Ed*. **1999**, *38*, 1747. (c) Labande, A.; Astruc, D. *Chem. Commun*. **2000**, 1007. (d) Alonso, E.; Labande, A.; Raehm, L.; Kern, J.-M.; Astruc, D. *C. R. Acad. Sci., Ser. 2c* **1999**, *2*, 209. (e) Daniel, M.-C.; Ruiz, J.; Nlate, S.; Palumbo, J.; Blais, J.-C.; Astruc, D. *Chem. Commun*. **2001**, 2000.

10.1021/ja017015x CCC: $22.00

functional alkanethiol−gold colloids containing a mixture of alkanethiol ligands and (amidoferrocenyl)alkanethiol (AFAT) ligands and monitored the titration of *n*-Bu_4N^+ salts of $H_2PO_4^-$ and HSO_4^- by these colloids using cycling voltammetry. Recognition of anions is an important topic because a number of anions are found in biology.[7,8]

Beer has shown that amidoferrocenyl groups linked to various endo-receptors are able to sense anions.[8] We have also disclosed the recognition of $H_2PO_4^-$, HSO_4^-,[6a] and Cl^- and Br^- [6b] by metallodendrimers. From preliminary studies, we know that the redox potential of the amidoferrocenyl group is sufficiently perturbed by the synergy between the H-bonding, electrostatic interaction, and topography in alkanethiol−gold nanoparticles containing AFAT ligands (unlike in alkylamidoferrocene monomers) to recognize $H_2PO_4^-$ and HSO_4^-.[6c] The detailed results of this study are reported here with thiol ligands containing amidoferrocene termini (AFAT ligands). In particular, we have also synthesized and stabilized on gold nanoparticles new thiol ligands containing branches that were modified using a C_5Me_5 or a C_5H_4COMe ring in the ferrocenic frame to investigate the role of the stereoelectronic factors on the recognition sites. Various alkanethiols functionalized with ferrocenyl termini were already synthesized, mainly for electron-transfer studies on self-assembled monolayers. For instance, amidoferrocenyl−alkanethiol ligands are known from Creagers' work.[9,10] The thiols containing *functionalized* ferrocenyl groups introduce the *supramolecular* character that had not been exploited and allowed us to develop the study of the *molecular-recognition properties*. Ligand-substitution reactions in alkanethiol−gold nanoparticles of Brust type are known with other alkanethiol ligands including ferrocenylalkanethiol ligands, and it was shown that the gold core was unchanged during such reactions.[11] Recently, Nishihara synthesized nanoparticles containing thiol ligands that were terminated by mixed-valence biferrocenyl groups, bringing versatile redox properties to the nanoparticles.[12]

Results and Discussions

Gold Colloid Syntheses. The thiol-ligand syntheses are described in the Supporting Information. With the Cp* and $CpCOCH_3$ groups, however, they are shown in Schemes 1 and 2.

The gold colloids with dodecanethiol ligands were synthesized according to Brust's procedure.[4] The combination of elemental analysis, ^1H NMR, and TEM according to Leff's model[13] allowed us to determine an average number of 269 gold atoms/core of 2-nm diameter and 103 dodecanethiolate chains (see Experimental Section). These results are in agreement with those obtained by Brust with gold nanoparticules stabilized by dodecanethiol ligands.[4] Then, a variable proportion of AFAT ligands has been introduced by the ligand-exchange procedure used by Murray for other ligands.[11]

We have applied this technique with AFAT ligands of variable length (11 and 6 C atoms)[6c] and structure (Cp, Cp*, $CpCOCH_3$) and verified using TEM that the core size was not modified upon ligand substitution. Table 1 shows the proportion of AFAT ligands (determined by ^1H NMR) that is introduced onto the nanoparticles as a function of the amount engaged in the ligand-substitution reactions (Scheme 3).

In particular, with (amidoferrocenyl)undecanethiol ligands, saturation is reached for 38 AFAT ligands/particle. Reactions carried out in the presence of larger amounts of AFAT ligands never gave a content higher than 38% AFAT ligands in the mixed colloids, which is in accord with Murray's investiga-

Scheme 1. Synthesis of the 11-(1-Amido,1′-pentamethylferrocenyl)-1-undecanethiol Ligand **12**

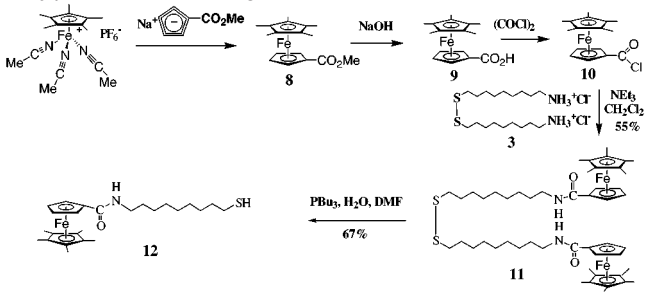

Scheme 2. Synthesis of the 11-(1-Amido,1′-acetylferrocenyl)-1-undecanethiol Ligand **15**

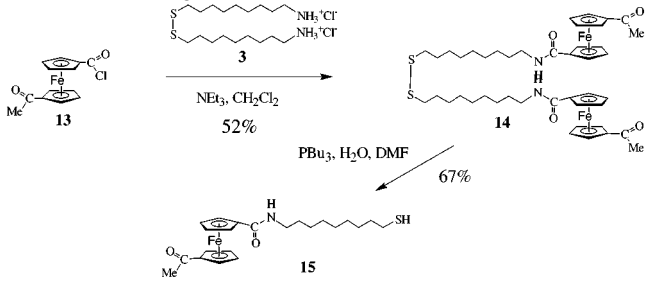

Table 1. Results of Ligand-Exchange Reactions between AFAT and Dodecanethiol (DT) Gold Nanoparticles

AFAT chain length	AFAT/DT ratio		AFAT/DT nos. in product[c]	% AFAT in product[d]
	reacn[a]	product[b]		
C11	1:4	1:13	8/97	7-Fc
C11	1:1	1:8	10/70	13-Fc
C11	1.5:1	1:5	21/85	20-Fc
C11	1.75:1	1:3.5	31/75	29-Fc
C11	2:1	1:2.6	39/64	38-Fc
C6	2:1	1:5.5	16/70	18-Fc

[a] Mole ratio of AFAT ligand to nanoparticle-bound dodecanethiolate (DT) ligands in ligand-exchange reactions. [b] Average mole ratio AFAT/DT ligands obtained in the nanoparticles. [c] Average numbers of AFAT/DT ligands obtained in the particles. [d] Average % of AFAT ligands obtained in the nanoparticles.

(7) Seel, C.; de Mendoza, J. In *Comprehensive Supramolecular Chemistry*; Atwood, J., Davies, J. E. D., McNichol, D. D., Vögtle, F., Eds.; Elsevier: New York, 1996; Vol. 2, Chapter 17, pp 519−552.
(8) (a) Beer, P. D. *Adv. Inorg. Chem.* **1992**, *39*, 79. (b) Beer, P. D. *J. Chem. Soc., Chem. Commun.* **1996**, 689. (c) Beer, P. D. *Acc. Chem. Res.* **1998**, *31*, 71. (d) Beer, P. D.; Gale, P. A.; Chen, Z. *Adv. Phys. Org. Chem.* **1998**, *31*, 1. (e) Beer, P. D.; Gale, P. A. *Angew. Chem., Int. Ed.* **2001**, *40*, 486.
(9) (a) Weber, K.; Creager, S. E. *Anal. Chem.* **1994**, *66*, 3164. (b) Rowe, G. K.; Creager, S. E. *J. Phys. Chem.* **1994**, *98*, 5500. (c) Weber, K.; Hockett, L.; Creager, S. E. *J. Phys. Chem. B* **1997**, *101*, 8286. (d) Creager, S.; Yu, C. J.; Bamdad, C.; O'Connor, S.; MacLean, T.; Lam, E.; Chong, Y.; Olsen, G. T.; Luo, J.; Gozin, M.; Kayyem, J. F. *J. Am. Chem. Soc.* **1999**, *121*, 1059.
(10) For esters, see: Chidsey, C. E. D.; Bertozzi, C. R.; Putvinski, T.; Mujsce, A. M. *J. Am. Chem. Soc.* **1990**, *112*, 4301.
(11) (a) Hosteler, M. J.; Green, S. J.; Stockes, J. J.; Murray, R. W. *J. Am. Chem. Soc.* **1996**, *118*, 4212. (b) Ingram, R. S.; Hostetler, M. J.; Murray, R. W. *J. Am. Chem. Soc.* **1997**, *119*, 9175. (c) Hostetler, M. J.; Templeton, A. C.; Murray, R. W. *Langmuir* **1999**, *15*, 3782. (d) Templeton, A. C.; Wuelfing, W. P.; Murray, R. W. *Acc. Chem. Res.* **2000**, *33*, 27.
(12) (a) Horikoshi, T.; Itoh, M.; Kurihara, M.; Kubo, K.; Nishihara, H. *J. Electroanal. Chem.* **1999**, *473*, 113. (b) Yamada, M.; Tadera, T.; Kubo, K.; Nishihara, H. *Langmuir* **2001**, *17*, 2263. (c) Yamada, M.; Quiros, I.; Mizutani, J.; Kubo, K.; Nishihara, H. *Phys. Chem. Chem. Phys.* **2001**, *3*, 3377. (d) Men Y., Kubo, K.; Kurihara, M.; Nishihara, H. *Phys. Chem. Chem. Phys.* **2001,** *3*, 3427.
(13) Leff, D. V.; Ohara, P. C.; Heath, J. R.; Gelbart, W. M. *J. Phys. Chem.* **1995**, *99*, 7036.

Scheme 3. Ligand Substitution Reactions (CH_2Cl_2, 2 d, RT) for the Syntheses of the Gold Colloids Containing Mixed Dodecanethiol and AFAT-Type Ligands with Variation of the Chain Length (C_{11} vs C_6) and Ring Structure of the Ferrocenyl Motif (Cp, Cp*, C_5H_4COMe)

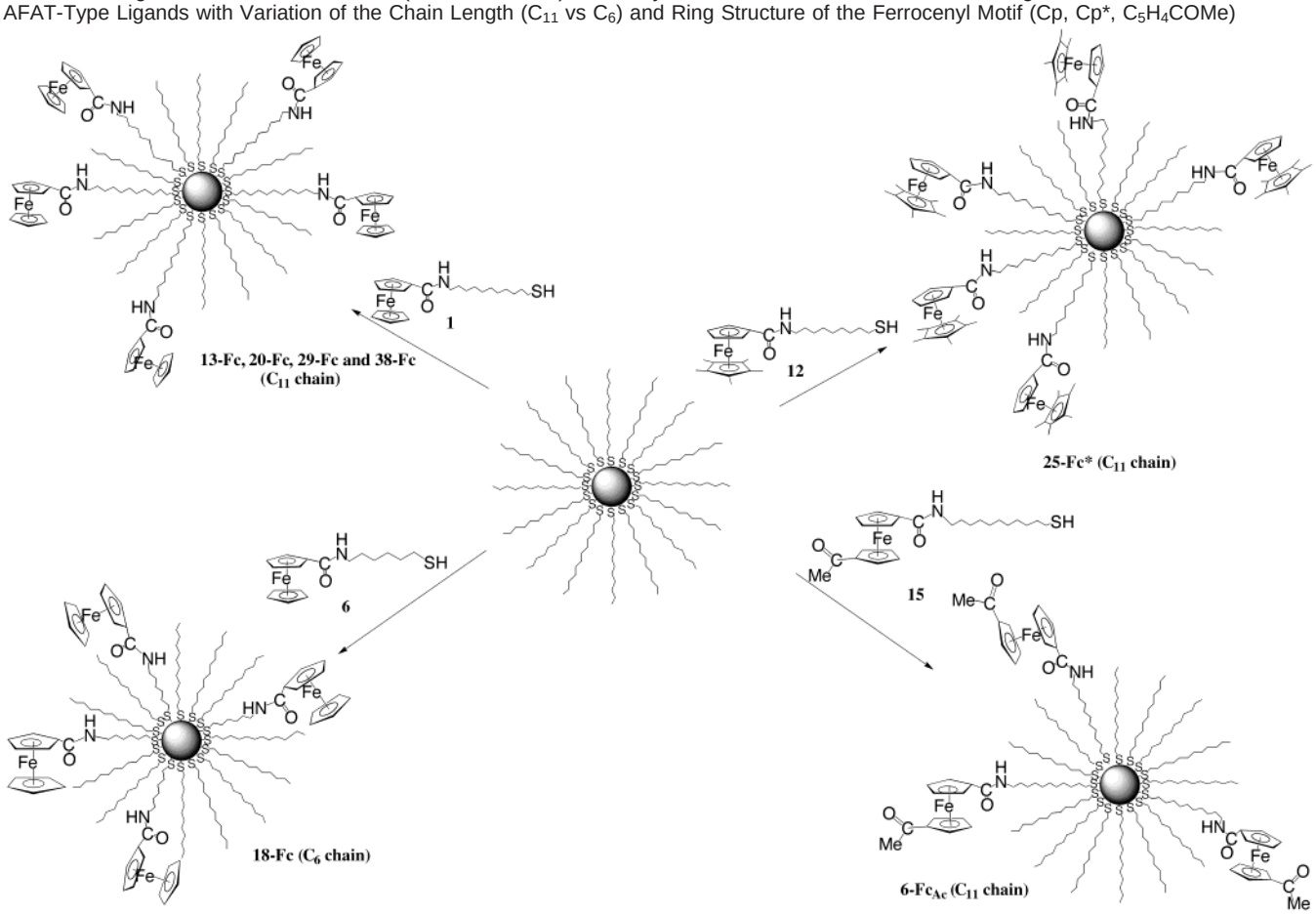

tions.[11] These nanoparticles are stable in air and thermally, and they are soluble in CH_2Cl_2. They are not soluble in polar solvents, however, which limits the range of conditions for the recognition studies.

Only 18% of **6** was introduced on the colloid starting from 2-fold excess of this ligand vs dodecanethiol whereas 25% of **12** was introduced starting from an excess of 1.7/1.

The ligand substitution with (1-amido,1′-acetylferrocenyl)-undecanethiol ligands was carried out using 1.1 equiv of this ligand (carefully reduced from the disulfide) vs dodecanethiol ligands. This resulted in the introduction of only 6% of ((1-amido,1′-acetyl)ferrocenyl)undecanethiol ligands starting from 1.1 equiv of **15**/dodecanethiol ligand. The polarity of the acetyl group of **15** lowers the solubility of the colloids in nonpolar solvents, which inhibits further ligand substitution. This proportion of redox-active ligand is sufficient for electrochemistry and recognition studies, however. The core size (2.1 ± 0.5 nm in average measured by HRTEM; 270 ± 70 gold atoms) and ligand number (103 ± 25) are essentially unchanged in these reactions. Various proportions of AFAT ligands **1** have been introduced depending of the amount engaged in the exchange reaction (see Table 1; saturation is reached at 38-Fc for the C_{11} chain ligands **1** and 18-Fc for the C_6-chain ligand **6**). A 1.7 equiv amount of the ligand 11-(1-amido,1′-pentamethylferrocenyl)-1-undecanethiol ligand **12** yielded 25-Fc* colloids, i.e. containing 25% of this ligand.

Cyclic Voltammetry of the Colloids. The cyclic voltammograms (CVs) were recorded using classic conditions (Pt, CH_2Cl_2, 0.1 M [n-Bu_4N][PF_6]). As for previously reported nanoparticles bearing ferrocenyl termini,[11,12] a single reversible ferrocene/ferrocenium wave was obtained with all the colloids bearing a proportion of thiol ligands with an amidoferrocenyl termini or one of its derivatives whose structure and syntheses are described above. The shape of this wave varies and depends on the exact nature of the ferrocene termini, but the following common features are observed. The cathodic return wave is, in general, higher and thinner than the anodic forward wave, which can be attributed to some adsorption of the colloids onto the electrode surface in the ferrocenium form. The difference between the anodic and cathodic peak potentials (ΔE_p) is always lower than the 58-mV value expected for a reversible single-electron wave of an electroactive species in solution at 20 °C:[14] the ΔE_p values are in the range of 20−30 mV, which also means that some adsorption occurs (the fully adsorbed redox species would ideally have a nil ΔE_p value). The observation of a single wave means that, in principle, all the redox sites are equivalent on the electrochemical time scale. One may note that since the rotation of the colloidal particles must be much faster than the electrochemical time scale, the location of all the redox sites vs the electrode is, on average, similar. In particular, there is no redox site for which a slow electron transfer is disclosed.[15−17]

(14) Bard, A. J.; Faulkner, R. L. *Electrochemical Methods*; Wiley: New York, 1980.
(15) (a) Gorman, C. B.; Parkhurst, B. L.; Su, W. Y.; Chen, K.-Y. *J. Am. Chem. Soc.* **1997**, *119*, 1141. (b) Gorman, C. B. *Adv. Mater*. **1997**, *9*, 1117; **1998**, *10*, 295. (c) Gorman, C. B.; Smith, J. C.; Hager, M. W.; Parkhurst, B. L.; Sierzputowska-Gracz, H.; Haney, C. A. *J. Am. Chem. Soc.* **1999**, *121*, 9958.

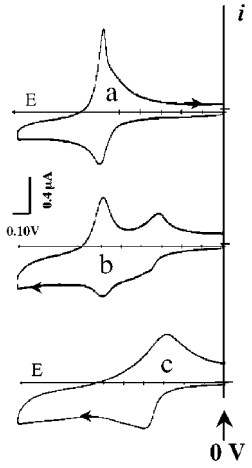

Figure 1. Cyclic voltammograms of the gold nanoparticles 38-Fc: solvent, CH_2Cl_2; reference electrode, aqueous SCE; working and counter electrode, Pt; supporting electrolyte, 0.1 M *n*-Bu_4NPF_6; scan rate, 200 mV·s^{-1}. Key: (a) without [*n*-Bu_4N][H_2PO_4]; (b) with 0.6 equiv of [*n*-Bu_4N][H_2PO_4]/amidoferrocenyl branch; (c) with excess [*n*-Bu_4N][H_2PO_4]. Independently, the $E_{1/2}$ values (see text) were determined using decamethylferrocene as an internal reference: [$FeCp^*_2$]/[$FeCp^*_2$] ($E^{o\prime} = -0.070$ V vs SCE on Pt in CH_2Cl_2).

Such a slow electron transfer could be caused by a location remote from the electrode. On the other hand, a difference in location of the various redox sites vs the electrode is awaited for colloidal particles adsorbed on the electrode surface, but a hoping mechanism among the ferrocenyl redox sites may then establish this equivalence.

The standard redox potential $E°$ is estimated from the average values of the anodic and cathodic waves [$E_{1/2} = (E_{pa} + E_{pc})/2$], although the adsorption causes a small error. Decamethylferrocene, actually a better reference than ferrocene,[18] can be used as universal reference. The $E_{1/2}$ values are 0.665 V with the AFAT ligands, 0.680 V with the C_6-chain ligands, 0.365 V with Cp*, and 0.750 V with $CpCOCH_3$ (all values vs Cp_2*Fe, i.e. −0.545 V vs Cp_2Fe in CH_2Cl_2).

Recognition of $H_2PO_4^-$ and HSO_4^- by the Redox-Active Colloids. (a) Recognition and Titration of $H_2PO_4^-$. Addition of [*n*-Bu_4N][H_2PO_4] to a CH_2Cl_2 solution of these nanoparticles provokes the appearance of a new, cathodically shifted wave whose intensity increases at the expense of the initial wave. As for the initial wave, the new wave shows some adsorption and is characterized by a larger peak-to-peak separation than the standard 60-mV value for a reversible wave. This trend is characteristic of a relatively slow heterogeneous electron transfer due to a structural reorganization of the amidoferrocenyl−H_2PO_4 complex in the course of the redox change. The replacement of the initial wave by the new one is complete after addition of approximately 1 equiv of [*n*-Bu_4N][H_2PO_4]/AFAT branch (Figure 1), indicating a one-to-one interaction between the anion and the amidoferrocenium group, as proposed by Beer for receptors containing amidoferrocenyl groups (Chart 1).

Despite the perturbation caused by the adsorption phenomena and the slow heterogeneous electron transfer observed for the

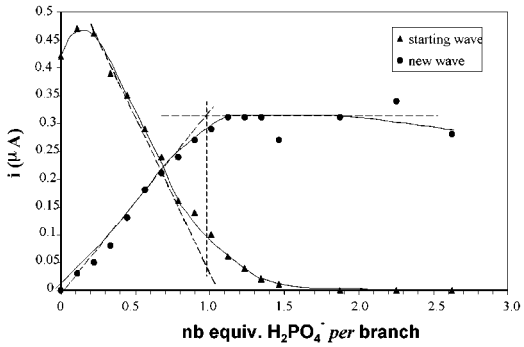

Figure 2. Titration of [*n*-Bu_4N][H_2PO_4] with the 20-Fc (AFAT) gold nanoparticles monitored by CV: decrease of the intensity of the initial CV wave (▲) and increase of the intensity of the new CV wave (●) vs the number of equivalents of [*n*-Bu_4N][H_2PO_4] added/AFAT branch. Nanoparticles: 5×10^{-6} M in CH_2Cl_2. [*n*-Bu_4N][H_2PO_4]: 10^{-2} M in CH_2Cl_2. [*n*-Bu_4N][PF_6]: 0.1 M. *T*: 20 °C. Reference electrode: SCE. Auxiliary and working electrodes: Pt. Scan rate: 200 mV·s^{-1}.

Chart 1. Double Hydrogen-Bonding Interaction between Amidoferrocenium and $H_2PO_4^-$

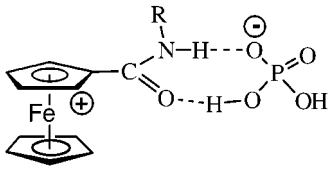

new wave, it is possible to carry out a titration using the disappearance of the initial wave and the appearance of the new wave. For this purpose, the variations of the intensities of the initial wave and the new wave are recorded as a function of the number of equivalents of [*n*-Bu_4N][H_2PO_4] added/amidoferrocenyl branch (Figure 2). These results are obtained with gold nanoparticles containing various proportions of AFAT ligands. For instance, Figure S1 (Supporting Information) compares the titration with various proportions of AFAT ligands.

It is remarkable that the potential shift resulting from the addition of the *n*-Bu_4N^+ salt of the anion $H_2PO_4^-$ is large ($\Delta E_{1/2} = 220 \pm 20$ mV). It is also almost constant upon variation of the proportion (from 8 to 38%) and length (11 vs 6 CH_2 units) of AFAT ligands in the nanoparticles. This trend is different from that observed with amidoferrocenyl dendrimers for which the potential shift dramatically increases with the dendrimer generation [potential shift in CH_2Cl_2 upon addition of 1 equiv of $H_2PO_4^-$ anion: 45 mV (1-Fc); 110 mV (3-Fc); 220 mV (9-Fc); 315 mv (18-Fc)].[6,18b] Thus, the mixed alkanethiol/AFAT colloids seem to be about as efficient as the nonakis(amidoferrocenyl) dendrimer. The phenomenum is also comparable to that obtained for the same C_{11} AFAT ligand alone at a gold electrode in a preliminary study (coverage, $\tau = 36\%$; potential shift, 290 mV; $E_{pa} - E_{pc} = 150$ mV for the new wave; the redox system is not stable more than a few cycles, however).[6d] According to the seminal Echegoyen−Kaifer model,[19] the replacement of a wave by another one due to interaction with one of the redox states corresponds to the square Scheme 4.

In this model, the interaction of the host is strong with one of the redox forms and weaker (but significant) with the other, the ratio of apparent association constants being

$$E°_{free} - E°_{bound} = \Delta E° \text{ (V)} = 0.058 \log (K_{(+)}/K_{(0)}) \text{ at } 20 \text{ °C}$$

This $\Delta E_{1/2}$ (value close to $\Delta E°$) corresponds to the apparent association constant $K_{(+)}$ between $H_2PO_4^-$ and the polyferro-

(16) Green, S. J.; Pietron, J. J.; Stockes, J. J.; Hosteler, M. J.; Vu, H.; Wuelfing, W. P.; Murray, R. W. *Langmuir* **1998**, *14*, 5612.
(17) (a) For a recent review of electron transfer in and supramolecular electrochemistry of nanosized assemblies containing many ferrocenyl centers, see: Kaifer, A. E.; Gomez-Kaifer, M. *Supramolecular Electrochemistry*; Wiley-VCH: Weinheim, Germany, 1999; Chapter 16, p 207. (b) Cardona, C. M.; Kaifer, A. E. *J. Am. Chem. Soc.* **1998**, *120*, 4023.

Scheme 4. Square Scheme Relating the Apparent Association Constants between the Oxoanionic Guest and Colloids under the Neutral Amidoferrocenyl Form ($K_{(0)}$) and the Amidoferrocenium Form ($K_{(+)}$) to the Standard Redox Potentials of the Free and Bound Forms ($E°_{free}$ and $E°_{bound}$, Respectively)

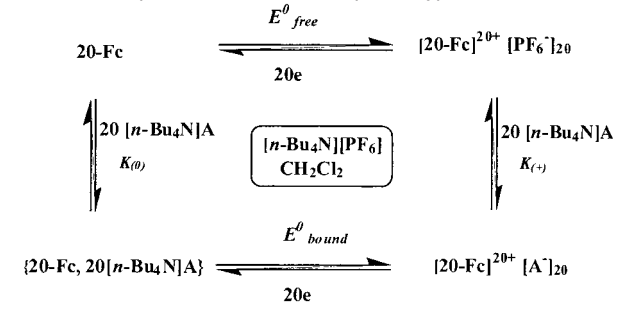

cenium form of the nanoparticles that is 6210 ± 620 times larger than that, $K_{(0)}$, related to the neutral polyferrocene form (electrostatic effect).[8,19] The fact that the interaction of $H_2PO_4^-$ is so much stronger with the amidoferrocenium form than with the amidoferrocenyl one signifies that the hydrogen bonding between the negatively charged oxygen atom of this anion and the positively charged −NH− group is the dominant one. The reason thereof is that this positive charge is largely enhanced upon oxidation of the ferrocenyl group.

The new wave always appears whatever the structure of the amidoferrocene termini of the thiol ligand, i.e. whether it bears electron-releasing or electron-withdrawing substituents. However, the potential shift very much depends on the detailed stereoelectronic features of the amidoferrocene termini (Figure S1 and S2, Supporting Information).

By comparison with the parent AFAT ligand, the AFAT ligand bearing a Cp* ring induces a smaller potential shift of 125 mV, which corresponds to an apparent association constant ratio $K_{(+)}/K_{(0)} = 143 \pm 15$ that is 50 times smaller than with the parent AFAT ligands. The steric constraints brought about by the ring permethylation disfavor the interaction between the amido group and the dihydrogenophosphate anion. The electronic effect is also clear since electron-releasing groups lower the positive charge at the NH group responsible for the main H-bonding leading to the recognition. Thus, this dramatic decrease of potential shift is due to the addition of negative steric and electronic effects. On the other hand, the potential shift recorded with the amidoferrocenyl termini bearing an acetyl substituent in larger (275 ± 10 mV) than that observed with the parent AFAT ligand. This potential shift means that the apparent association constant $K_{(+)}$ of the anion with the colloid bearing the cationic ferrocenium form of the electroactive (1-acetyl,1′-amidoferrocenyl)dodecanethiolate ligand is 55 130 ± 5500 times larger than that ($K_{(0)}$) of the anion with the colloid bearing the neutral Fe^{II} form of the same ligand. This ratio is nine times larger than with the parent AFAT ligand. Thus, the compared effects of the ligands modified with the Cp* and acetyl-Cp ligands respectively are in agreement given their opposite electronic characters. These results may be taken into account, with the electron-accepting acetyl substituent, by a larger electrostatic interaction between the anion and the ferrocenium centers when this center is more electron poor and by the larger value of the positive charge on the NH atoms of the amido group. This analysis also shows that, within the chelating hydrogen-bonding interactions, the hydrogen bond of this NH group with the oxygen atom of the $H_2PO_4^-$ anion is more significant than that between the oxygen atom of the amido group and the OH group of $H_2PO_4^-$. The remarkable influence of the stereoelectronic effect shows the importance the geometric and electronic conditions in the weak supramolecular interactions leading to recognition. Thus, the channels defined between the parallel ligands create sufficient steric strain to provide a favorable particle effect comparable in some way to the dendritic effect obtained with metallodendrimers.[18b,20]

Table 2. Determination of the Average Number of AFAT Ligands in the Nanoparticles in CH_2Cl_2

	total no. of AFAT ligands			
		titration by CV		
% AFAT	^{1}H NMR	$H_2PO_4^-$	$H_2PO_4^-$ [a]	HSO_4^-
8-Fc (C11)	8	8.3		
13-Fc (C11)	10	9.5	9	10.25
20-Fc (C11)	21	22	19	18
29-Fc (C11)	31	29	25	17[b]
38-Fc (C11)	39	32	29.5	13[b]
18-Fc (C6)	16	14		9[b]

[a] Titration carried out in the presence of excess [*n*-Bu_4N][HSO_4] (5×10^{-6} mol) and *n*-Bu_4NCl (2.5×10^{-6} mol). [b] Low value due to intramolecular H-bonding at high content of AFAT ligand (see text and Experimental Section).

This titration technique also allows one to confirm the number of AFAT ligands in the particles determined by ^{1}H NMR for the gold nanoparticles containing a proportion of AFAT ligands in the range 13%−29% (Table 2).

(b) Recognition and Titration of HSO_4^-. Addition of [*n*-Bu_4N][HSO_4] to a CH_2Cl_2 solution of these gold nanoparticles containing dodecanethiol and AFAT ligands or AFAT ligands modified with Cp* provokes the progressive shift of the initial CV wave, a behavior completely different from that observed upon addition of [*n*-Bu_4N][H_2PO_4]. This progressive shift stops when approximately 1 equiv of [*n*-Bu_4N][HSO_4]/redox active ligand has been added in the case of nanoparticles containing a low percentage of AFAT ligands (8−20%). The potential shift is rather weak, and its value is 30 ± 5 mV in average with the parent AFAT ligands. Using the Cp* ring instead of the Cp one led to a potential shift of 25 ± 5 mV. The potential shift is weaker than that recorded with the amidoferrocenyl dendrimers [no significant shift (1-Fc), 30-mV (3-Fc), 65 mV (9-Fc), 130 mV (18-Fc)],[6a,b] whereas no potential shift was observed with the gold electrode modified with the C_{11}-AFAT ligand.[6d] In the Kaifer−Echegoyen model, this corresponds to the square scheme above but with weak interaction between the host and the reduced form ($K_{(0)} \ll 1$). Under these conditions, there is, according to this model, a direct access to the absolute value of the apparent association constant $K_{(+)}$: $\Delta E°$ (V) = 0.058 log $K_{(+)}c$ at 20 °C, c being the concentration of added anion.

This corresponds to an apparent association constant $K_{(+)} = 400 \pm 100$ $mol^{-1}\cdot L$ at a concentration of 10^{-2} M of AFAT

(18) (a) Ruiz, J.; Astruc, D. *C. R. Acad. Sci. Paris, Ser. 2c* **1998**, 21. (b) Astruc, D. In ref 3b, Chapter 4, p 728.
(19) Seminal report: Miller, S. R.; Gustowski, D. A.; Chen, Z.-H.; Gokel, G. W.; Echegoyen, L.; Kaifer, A. E. *Anal. Chem.* **1988**, *60*, 2021.
(20) (a) Newkome, G. R.; He, E.; Moorefield, C. N. *Chem. Rev.* **1999**, *99*, 1689. (b) Balzani, V.; Campagna, S.; Denti, G.; Juris, A.; Serroni, S.; Venturi, M. *Acc. Chem. Res.* **1998**, *31*, 26. (c) Cuadrado, I.; Morán, M.; Casado, C. M.; Alonso, B.; Losada, J. *Coord. Chem. Rev.* **1999**, *189*, 123. (d) Hearshaw, M. A.; Moss, J. R. *Chem. Commun.* **1999**, 1. (e) Astruc, D.; Chardac, F. *Chem. Rev.* **2001**, *101*, 2991.

Chart 2. Possible Interactions between Amidoferrocenium and HSO_4^- Involving Various Amounts of Equivalents of HSO_4^-

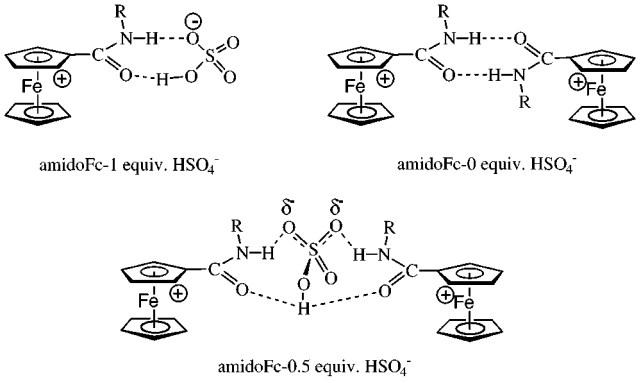

ligand (with Cp*, $\Delta E_{1/2} = 25$ mV; $K_{(+)} = 270 \pm 70$ mol^{-1}·L). It is noteworthy that the $\Delta E_{1/2}$ value is much smaller for HSO_4^- than for $H_2PO_4^-$, which is consistent with the selectivity of the recognition by these nanoparticles (vide infra).

With the AFAT ligand modified with Cp*, the value of the potential shift $\Delta E_{1/2}$ is even lower, only 25 mV, which corresponds to an apparent association constant $K_{(+)} = 270 \pm 70$ mol^{-1}·L. The titration was carried out only with the 25-Fc* colloids for which $\Delta E_{1/2} = 27.5 \pm 5$ mV, which is the limit of the possibility given the high percentage of error. This very low $\Delta E_{1/2}$ value is due to the decreased hydrogen-bonding interaction, electrostatic effect, and steric constraints with the Cp* modification compared to the parent AFAT ligand, already mentioned above for $H_2PO_4^-$.

The weaker interaction of the amidoferrocenium group with the HSO_4^- anion than with the $H_2PO_4^-$ anion can be taken into account by the lower charge density on the oxygen atom in the former. This is due to the facts that the negative charge is delocalized onto three oxygen atoms in HSO_4^- instead of only two in $H_2PO_4^-$ and that sulfur is more electronegative than phosphorus (Pauling electronegativity indices: 2.6 and 2.2, respectively). Thus, $H_2PO_4^-$ is more basic than HSO_4^- in CH_2Cl_2. On the other hand, HSO_4^- is more acidic than $H_2PO_4^-$, but this property does not dominate because the amidic oxygen atom has little basicity in the amidoferrocenium form. The compared recognition experiments for these two anions indeed confirm that the dominant hydrogen-bonding interaction involves the −NH− group of the amide and a terminal oxygen atom of the anions.[8] When the proportion of AFAT ligands is large (in 29-Fc and 38-Fc) or the chain short (C_6), however, the equivalence point is no longer reached after addition of 1 equiv of HSO_4^- anion/amidoferrocenyl branch but near 0.5 equiv of HSO_4^-. This effect is even more marked with the Cp* modification of the AFAT ligand for which the equivalent point was observed for only 0.7 equiv of HSO_4^- anion with the 25-Fc colloids. It is possible that the proportion of amidoferrocenyl dimers being higher given the parallelism of the ligands in the nanoparticles, the HSO_4^- anion cannot compete with their formation. Note along this line, in comparison, that the AFAT ligand alone on a gold electrode does not sense the HSO_4^- anion at all.[6d] Another possibility is that the HSO_4^- anion bridges two neighboring amido groups (Chart 2).

Accordingly, this effect is also more marked for HSO_4^- than for $H_2PO_4^-$. The HSO_4^- anion−amidoferrocenyl branch interaction is weak in the AFAT-containing colloids and is thus the subject of perturbations due to any relatively low-energy event. Figure 4 illustrates the fact that the titration is clear, however. Despite the low ΔE value, it is thus possible to titrate [*n*-Bu_4N][HSO_4] using the nanoparticles that have a low content of AFAT ligands (8−20%).

The accuracy is better with a higher content of AFAT ligand than with a low one. Thus, the best choice is a compromise with 13-Fc, i.e. a proportion of 13% AFAT ligands in the colloids (see Table 4).

The use of the acetylcyclopentadienyl variation of the AFAT ligand offers the possibility of a stronger interaction with the HSO_4^- anion. Interestingly, a new event is observed in this case upon addition of the HSO_4^- anion to the 6-Fc_{Ac}. A new wave appears at a peak potential $E_{pc} = 170$ mV more positive than that of the original wave, but this new wave is not reversible; i.e., the corresponding anodic wave is almost absent (weak

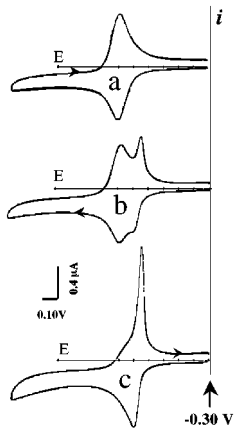

Figure 3. Cyclic voltammograms of the gold nanoparticles 25-Fc* during titration with $H_2PO_4^-$: solvent, CH_2Cl_2; reference electrode, aqueous SCE; working and counter electrode, Pt; supporting electrolyte, 0.1 M *n*-Bu_4NPF_6; scan rate, 200 mV·s^{-1}. Key: (a) without [*n*-Bu_4N][H_2PO_4]; (b) with 0.75 equiv of [*n*-Bu_4N][H_2PO_4]/1-amido,1′-pentamethylferrocenyl branch; (c) with excess [*n*-Bu_4N][H_2PO_4].

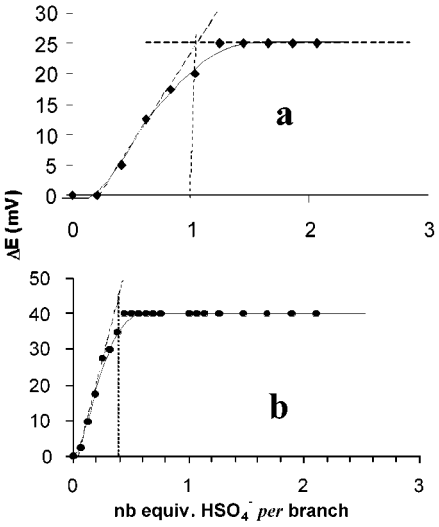

Figure 4. Titration of [*n*-Bu_4N][HSO_4] by gold nanoparticles containing AFAT ligands in CH_2Cl_2, showing shift of $E_{1/2}$ toward positive potentials as a function of the number of equivalents of [*n*-Bu_4N][HSO_4] added/amidoferrocenyl branch of the colloids. See Figures 1 and 2 and Experimental Section for conditions. Key: (a) titration by 13-Fc, where the equivalence point is 1 equiv of [*n*-Bu_4N][HSO_4]/amidoferrocenyl branch; (b) titration by 38-Fc, where the equivalence point is 0.4 equiv of [*n*-Bu_4N]-[HSO_4]/amidoferrocenyl branch.

Table 3. Potential Shift $\Delta E_{1/2}$ Observed for the $Fe^{II/III}$ Redox System upon Addition to the Colloids of 1 equiv of Anion/Amidoferrocenyl Branch during Titrations of $H_2PO_4^-$, HSO_4^-, and $H_2PO_4^-$ in the Presence of both [*n*-Bu_4N][HSO_4] and [*n*-Bu_4N]Cl[a]

	$\Delta E_{1/2}$ (mV)		
% AFAT	$H_2PO_4^-$	equiv of H_2PO_4 with HSO_4^- and Cl^-	HSO_4^-
8-Fc (C11)	200 ± 20		25 ± 10
13-Fc (C11)	240 ± 20	112 ± 15	32 ± 10
20-Fc (C11)	215 ± 20	100 ± 15	27 ± 10
29-Fc (C11)	200 ± 20	125 ± 15	37 ± 10
38-Fc (C11)	232 ± 20	175 ± 20	30 ± 10

[a] See the captions to Figures 1 and 2 for conditions.

shoulder). This could be the indication that the interaction between the HSO_4^- anion and the 6-Fc_{Ac} colloids is strong in the ferrocenium form and almost too weak to be significant in the neutral form. The practical consequence is that the thermodynamic potential corresponding to the new wave is not accessible with a reasonable accuracy. Another problem is that the percentage of 11-(amido(acetylferrocenyl))-1-undecanethiol ligand in the colloid is very low (6%). This latter aspect disfavors the accuracy in titrations. Such a titration has been best carried out, however, by measurement of the variation of intensity the new wave. The accuracy of the titration is only of the order of 10−20% of the number of equivalents of HSO_4^- anion, which is confirmed by the slightly too large value of 1.1 equiv of HSO_4^- anion observed.

(c) Other Anions. Finally, these particles do not recognize the chloride, bromide, and nitrate anions, the potential shift being nil or nonsignificant upon addition of a [*n*-Bu_4N] salt of these anions. Further work with other supramolecular systems and techniques is underway for these anions.

(d) Titration of [*n*-Bu_4N][H_2PO_4] in the Presence of both [*n*-Bu_4N][HSO_4] and [*n*-Bu_4N]Cl: Selectivity. It was of interest to examine the behavior of the CV wave of the AFAT-containing colloids as a function of the addition of [*n*-Bu_4N][H_2PO_4] when other salts of anions were present in the solution. This type of study allows investigating the selectivity for the recognition of the $H_2PO_4^-$ anion. Thus, addition of [*n*-Bu_4N][H_2PO_4], when the salts [*n*-Bu_4N][HSO_4] and [*n*-Bu_4N]Cl (in addition to the electrolyte [*n*-Bu_4N][PF_6] in 2×10^4 fold excess) are present in solution in concentrations equal to that of the amidoferrocenyl ligands, does not lead to the appearance of a new wave at a less positive potential than the initial one. On the other hand, this addition leads to a progressive shift of the initial wave toward more positive potentials. This means that, contrary to the situation for which these salts are absent, it is now possible to titrate the $H_2PO_4^-$ anions by plotting the potential shift as a function of the addition of [*n*-Bu_4N][H_2PO_4]. We have carried out these titrations with the 13-Fc, 20-Fc, 29-Fc, and 38-Fc colloids, and the titration graphs led to equivalence points reached for 0.87, 0.82, 0.75, and 0.75 equiv of [*n*-Bu_4N][H_2PO_4], respectively (see Table 4 and Figure 5).

Thus, this equivalence point is approaching unity when the proportion of AFAT ligands becomes low. This difference of behavior when the other anions are present shows that there is competition and perturbation among the anions that interact with the amidoferrocenyl groups of the colloids. Nevertheless, the $H_2PO_4^-$ anion can be conveniently titrated. The shift of potential at the equivalence point vs the initial wave is 120 ± 10 mV

Table 4. Determination of the Number of Equivalents of Anion/Amidoferrocenyl Branch of the Colloids in the Titrations Using the Colloids with Various Proportions of AFAT Ligand (C11)[a]

% AFAT	equiv of $H_2PO_4^-$	equiv of H_2PO_4 with HSO_4^- and Cl^-	equiv of HSO_4^-
8-Fc (C11)	1.25		1.10
13-Fc (C11)	1.0	0.87	1.0
20-Fc (C11)	1.0	0.82	0.88
29-Fc (C11)	0.94	0.75	0.55
38-Fc (C11)	0.75	0.75	0.35

[a] See the caption to Figures 1 and 2 for conditions and text for discrepancies with respect to the one-to-one interaction (1 equiv/branch).

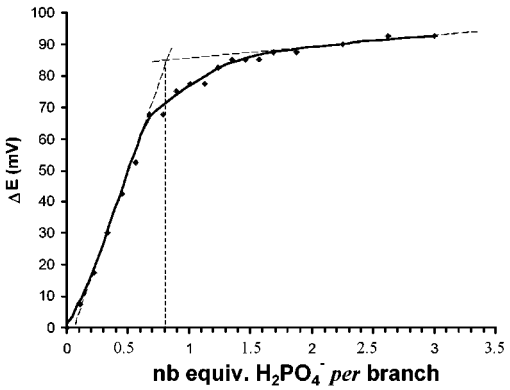

Figure 5. Titration of [*n*-Bu_4N][H_2PO_4] in the presence of both [*n*-Bu_4N][HSO_4] and [*n*-Bu_4N]Cl (in addition to the 2×10^4 excess of supporting electrolyte [*n*-Bu_4N][PF_6]) by 20-Fc gold nanoparticles in CH_2Cl_2, showing the shift of $E_{1/2}$ toward positive potentials as a function of the number of equiv of [*n*-Bu_4N][H_2PO_4] added/amidoferrocenyl branch of the 20-Fc colloids.

with the 13-Fc and 29-Fc colloids but reaches 175 mV with the more highly AFAT-loaded 38-Fc colloids (see Table 3). It is also noteworthy that the $E_{pa} - E_{pc}$ value increases from 20 to 200 mV in the course of the addition, which is again a characteristic of the relatively slow reorganization during the redox change. The shift of potential of the wave (instead of appearance of a new wave) when the other anions are present shows, according to the Kaifer−Echegoyen model, a much weaker interaction between the amidoferrocenyl groups and the $H_2PO_4^-$ anions in the presence of the other anions than in their absence. This is fully confirmed by the reduction of potential shift (120 mV instead of 220 mV). This shows that the *apparent* association constant $K_{(0)}$ becomes much weaker in the presence of the other anions, presumably because of the competition among the different anions in their interactions with the neutral amidoferrocenyl form of the AFAT ligands. The change of the association constant may be only apparent, however, at constant ionic strength. The observed change may in fact be the result of a dynamic equilibrium among the anion complexes. Despite this competition that considerably influences the recognition features, there is selectivity for the recognition of the $H_2PO_4^-$ anion. Although the potential shift is precisely the event observed with [*n*-Bu_4N][HSO_4] alone, the magnitude is considerably larger with [*n*-Bu_4N][HSO_4] + [*n*-Bu_4N]Cl + [*n*-Bu_4N][H_2PO_4] (120 mV) than with [*n*-Bu_4N][HSO_4] alone (30 mV). With the 38-Fc colloids, the significantly higher value of the potential shift indicates that the competition with the HSO_4^- anions is weaker, possibly because the HSO_4^- anions cannot disrupt the dimers formed between AFAT neighbors whereas the $H_2PO_4^-$ anions essentially do. In addition, the

increase of the $E_{pa} - E_{pc}$ value along the titration shows that the redox change of the amidoferrocenyl-branch anion involves some structural rearrangements whose kinetics is of the order of magnitude of the electrochemical time scale, i.e. rather slow. Such slow heterogeneous electron transfers are not found with the other anions alone, but they are characteristic of the rather strong amidoferrocenium branch$-H_2PO_4^-$ anion interaction. In the case of the shorter C_6 chain, however, no increase of the $E_{pa} - E_{pc}$ value was observed in the course of the titration, although the other features are as indicated above with the C_{11}-AFAT-containing chains. This could be the result of a weaker amidoferrocenium$-H_2PO_4^-$ interaction due to the buried character of this shorter-chain AFAT ligand. [12c]

In summary, the titration of the $H_2PO_4^-$ anions can be carried out in the presence of other anions, and the best choice is the colloids containing a proportion of 13% C_{11} AFAT ligands (see Table 4).

Concluding Remarks

The stereoelectronic effects of the Cp permethylation and Cp acetylation of the amidoferrocenyl group have a significant influence on the recognition properties that are weakened by Cp permethylation (electron releasing and sterically demanding) and enhanced by Cp acetylation (electron withdrawing). These results emphasize the key role, for the recognition by the amidoferrocenium form, of the H-bonding between the −NH− amido group and the charged terminal oxygen atom of the oxoanion.

One can titrate the oxoanions using either the decrease of the initial CV wave and the increase of the new wave at less positive potential ($H_2PO_4^-$) or the potential shift (HSO_4^-), the 13-Fc and 20-Fc colloids being the best choices for good results and accuracy. Moreover, it is also possible to titrate the $H_2PO_4^-$ anions in the presence of both [*n*-Bu_4N][HSO_4] and [*n*-Bu_4N]-Cl. This titration is characterized by a potential shift signifying an apparently lower $H_2PO_4^-$ anion−AFAT interaction due to the competition and perturbation by the other anions. The potential shift allows a convenient titration, ideally with the 13-Fc colloids.

Experimental Section

For general data, cyclic voltammetry, HRTEM, and ligand synthesis, see the Supporting Information.

Gold Colloids Functionalized with AFAT Ligands. Nanoparticles stabilized with dodecanethiolate ligands were synthesized by following the method described by Brust et al.[4] In a typical procedure, these gold nanoparticles (ca. 200 mg, 2.0 μmol) were dissolved in 100 mL of CH_2Cl_2 (concentrated in nanoparticles ca. 2 mg/mL). The solution was degassed and added under N_2 to the 11-(amidoferrocenyl)undecanethiol, which was stored in a dry Schlenk tube. The mixture was stirred at room temperature for 48 h under N_2. The solvent was evaporated to dryness, and the residue was washed thoroughly with methanol until the methanolic phase was colorless. The black solid was dried in vacuo. ^{1}H NMR ($CDCl_3$): δ (ppm) 4.68 (C*H* (C_5H_4CO)), 4.32 (C*H* (C_5H_4-CO)), 4.19 (C*H* (Cp)), 3.35 (C*H*$_2$NH), 1.26 (CH_2), 0.88 (CH_3). ^{13}C NMR ($CDCl_3$): δ (ppm) 170.3 (CO), 70.3 (*C*H C_5H_4CO), 69.7 (*C*H Cp), 68.2 (*C*H C_5H_4CO), 40.0 (CH_2NH), 33.0−30.0 (CH_2), 23.5 (CH_2), 15.0 (CH_2CH_3). Anal. Found for 8-Fc: Au, 69.42; S, 4.41. Calcd for Au/S: 2.56/1. Found for 13-Fc: Au, 69.24; S, 3.34. Calcd for Au/S: 3.37/1. Found for 20-Fc: Au, 63.37; S, 4.08. Calcd for Au/S: 2.53/1. Found for 29-Fc: Au, 61.35; S, 3.93. Calcd for Au/S: 2.54/1. Found for 38-Fc: Au, 57.37; S, 3.58. Calcd for Au/S: 2.61/1. Found for 18-Fc (C_6): Au, 69.19; S, 3.60. Calcd for Au/S: 3.13/1. Mean diameter of gold core for AFAT-functionalized gold nanoparticles (TEM.): D = 2.06 nm. Calculation of the number of gold atoms:[13] $N_{Au} = 4\pi R^3/3v_g = 4\pi(D/2)^3/51 = 269$. Calculation of the number of thiolate ligands $N_{th} = N_{Au}/(Au/S) = 269/2.61 = 103$. Molecular weight calculation (38-Fc): $Au_{269}(C_{12}H_{25}S)_{64}(SC_{11}H_{22}NHCOFc)_{39}$. Average M = 82035 g·mol^{-1}.

Gold Colloids Functionalized with 11-(1-Amido,1′-pentamethylferrocenyl)-1-undecanethiol, 7. The nanoparticles were synthesized according to the procedure described above. The black solid was dried in vacuo. ^{1}H NMR ($CDCl_3$): δ (ppm) 4.33 (CH (C_5H_4CO)), 3.84 (CH (C_5H_4CO)), 3.35 (CH_2NH), 1.83 (C_5CH_3), 1.25 (CH_2), 0.88 (CH_3). ^{13}C NMR ($CDCl_3$): δ (ppm) 169.2 (CO), 81.0 (C_5H_4CO), 74.2 (C_5H_4CO), 70.7 (C_5H_4CO), 39.8−39.2 (CH_2NH), 32.0−27.0 (CH_2), 22.7 (CH_2), 14.1 (CH_2CH_3), 10.6 (C_5CH_3). Anal. Found: Au, 38.20; S, 2.32. Calcd for Au/S: 2.68/1. Mean diameter of gold core (measured by TEM): D = 2.56 nm.

Gold Colloids Functionalized with 11-(1-Amido,1′-acetylferrocenyl)-1-undecanethiol, 15. The colloids were synthesized according to the above procedure. The black solid was dried in vacuo. ^{1}H NMR ($CDCl_3$): δ (ppm) 4.74 (CH(C_5H_4CO)), 4.53 (CH(C_5H_4CO)), 4.34 (CH-(C_5H_4CO)), 3.36 (CH_2NHCO), 2.41 (CH_3CO)),1.67−1.25 (CH_2), 0.88 (CH_3). Anal. Found: Au, 53.56; S, 3.79. Calcd for Au/S: 2.30/1.

Titrations. The calculation method used for the titrations (with example of 38-Fc) is as follows. Quantity added into the CV cell: $m_{particles}$ = 5 mg; $M_{38-Fc\ particle}$ = 82035 g·mol^{-1}; $n_{particles} = m_{particles}/M = 6.095 \times 10^{-8}$ mol. Quantity of anion added in 5 mL of solution: c_{sol} = 0.01 M → $n_{sol} = 5 \times 10^{-8}$ mol. An addition of 5 mL of solution allows the complexation of 0.82 branch ($5 \times 10^{-8}/6.095 \times 10^{-8} = 0.82$). At the equivalence point (38-Fc), X/mL of solution of anion is added. $Y = (0.82X)/5$ amidoferrocenyl branches are complexed. It is considered that 1 equiv is reached when the number of AFAT branches found by ^{1}H NMR is reached. For 38-Fc, 1 equiv is reached for a number of AFAT ligands equal to 39. Data for the titration of H_2PO_4: number of branches at the equivalence point, $Y = (0.82 \times 193)/5 = 32$; Number of equivalents of $H_2PO_4^-$ added, 32/39 = 0.8.

Acknowledgment. We thank Michel Chambon (Bordeaux I) for the HRTEM measurements, Professor Jean-Claude Blais (Paris VI) for mass spectra, Victor Martinez (LCOO) for helpful discussions, and the Institut Universitaire de France (D.A.), the CNRS, the University Bordeaux I, and the Région Aquitaine (grant to A.L.) for financial support.

Supporting Information Available: Ligand syntheses (Schemes S1 and S2), additional references and comments on colloid syntheses, CV, and recognition (Figures S1 and S2), general data including cyclic voltammetry, ^{1}H and ^{13}C NMR spectra of the AFAT ligands and mixed alkanethiolate/AFAT gold colloids, and HRTEM pictures of the mixed gold colloids (PDF). This material is available free of charge via the Internet at http//pubs.acs.org.

JA017015X